

Development of a Unified Feed-Forward Control System for Robotic Mechanisms using Finite Element Approach

Daigoro Isobe¹, Kouji Yamanaka^{2*}

¹ Department of Engineering Mechanics and Energy, University of Tsukuba, 1-1-1 Tennodai Tsukuba-shi, Ibaraki 305-8573, Japan

² Graduate School, University of Tsukuba, 1-1-1 Tennodai Tsukuba-shi, Ibaraki 305-8573, Japan

e-mail: isobe@kz.tsukuba.ac.jp, e0201364@edu.esys.tsukuba.ac.jp

Abstract Dynamic equations used for feed-forward control of robotic mechanisms include interdependent variables between the constituting links, since they are normally evaluated in relative polar coordinates and in the dimension of torque. Accordingly, it will become highly complicated to derive inverse dynamics of closed-loop link systems, continuously transforming systems, or of flexible link systems. Consideration of dynamics is required to realize stable control of robotic systems, and many researchers have tried to deal with the dynamics by improving theories and methods against each system. Isobe, on the other hand, developed a completely new solution scheme for inverse dynamics called the parallel solution scheme, which can be commonly applied in different types of link systems such as open- or closed-loop mechanisms, or ones constituted with rigid or flexible link members. The scheme is developed using a finite element approach, handling the entire system as a continuum. By taking advantage of natural characteristics of the finite element method (FEM), i.e., the capability of expressing the behavior of each discrete element as well as that of the entire continuous system, local information such as nodal forces and displacements can be calculated in parallel. It evaluates the analyzed model in absolute Cartesian coordinates with the equation of motion expressed in dimension of force. The inverse dynamics is calculated using a matrix form relation to the nodal forces obtained by the finite element calculation. The matrix-form equations are divided individually into terms of force, transformation between coordinates, and length, which makes the scheme potentially higher in applicability and expansibility.

The scheme can not only deal with open- and closed-loop link systems independently, but it can also deal seamlessly with those that gradually change their forms and dynamics. There is also no need to revise the basic numerical algorithm of the scheme, regardless of the stiffness of the constituting link member. Particularly, it is considered to be valid for link systems with elastic members, since the calculation process of the scheme is based upon the finite element approach.

The main objective of this study is to verify the extensive ability of the scheme as a unified scheme, by carrying out inverse dynamics calculations on several types of rigid and flexible manipulators, along with applications to feed-forward control of various types of link systems and robotic mechanisms.

Key words: feed-forward control, link systems, robotic mechanisms, parallel solution scheme, finite element method

INTRODUCTION

Dynamic equations derived by general schemes, such as the Newton-Euler method or the Lagrangian method, include interdependent variables between the constituent links, since they are evaluated in relative polar coordinates and in the dimension of torque. Accordingly, it is highly complicated to derive the inverse dynamics of closed-loop link systems, continuously transforming systems, and flexible link systems. Nakamura and Ghodoussi proposed a systematic computational scheme of the inverse dynamics specified for closed-loop link systems, which was derived using d'Alembert's principle [1]. Sugimoto derived an equation of motion for closed-loop link systems by the motor algebra [2]. Nakamura and

Yamane developed a computational algorithm for the inverse and forward dynamics of open and closed kinematic chains, which can be applied seamlessly to the motion of any rigid link system without switching algorithms [3]. However, these methods are specified for rigid-body link systems, and users occasionally need to revise the methods or dynamic equations when the form or elasticity of the hardware system is changed.

An approach with a completely different viewpoint is described in this paper, which enables not only the inverse dynamics computation of any rigid link system, but also that of flexible link systems by the same procedure. Isobe and Nakagawa first attempted an application of the finite element method (FEM), a widely used computational tool for analyzing structures and fluids, to a control system of connected piezoelectric actuators, and achieved good control not only of the actuator itself but also of the entire system [4]. By taking advantage of the natural characteristics of the FEM, i.e., the capability of expressing the behaviour of each discrete element as well as that of the entire continuous system, local information such as nodal forces and displacements can be calculated in parallel. After finding that the FEM can be used as a control scheme of a continuum, Isobe implemented the FEM in a solution scheme of inverse dynamics for various types of link system [5-7]. The scheme is called the parallel solution scheme, since the nodal forces in discrete models are calculated in parallel from a mechanical point of view. In the scheme, the analyzed model is evaluated in absolute Cartesian coordinates with the equation of motion expressed in the dimension of force. The nodal forces are calculated incrementally in matrix form, which does not require any revision of the overall frame, and the variables forming the frame can be revised by simply changing the input data in the case of a physical change in the hardware system. The calculated nodal forces are then converted into joint torques using a matrix-form equation divided into terms of force, the transformation between the coordinates, and length. The structure of the algorithm makes it seamless in its application to different types of link system under various boundary conditions such as open- or closed-loop link systems. The scheme can also be applied to link systems with different values of flexural stiffness. For many years, considerable effort has been made to model [8-11] or even calculate the inverse dynamics [12] of robotic arms with elastic members. In contrast, the parallel solution scheme only requires a precise target trajectory that takes into account stiffness and damping.

There are two different versions of the parallel solution scheme for calculating the inverse dynamics of link systems. One version uses linear Timoshenko beam elements with a single integration point to explicitly express the center of gravity of links, and the other uses Bernoulli-Euler beam elements with two integration points to express the consistent mass distribution of the links. The former version is easier to compare with conventional dynamic equations since it explicitly expresses the center of gravity. The latter, on the other hand, has merits in accuracy, calculation time and stability. The latter version is described in this paper, and some numerical examples are shown for several types of link system. The scheme is also implemented in a control system to evaluate the performance under actual control with dynamics compensation, and some control applications are shown for several types of link system and a robotic arm.

PARALLEL SOLUTION SCHEME

In the parallel solution scheme, a link system consisting of motor joints and links, as shown in Fig. 1(a), is modeled and subdivided using finite elements. One method of modeling the system is to subdivide a link into two linear Timoshenko beam elements, as shown in Fig. 1(b), with an intermediate node at the center of gravity [6]. Another method is to substitute a link with a Bernoulli-Euler beam element, as shown in Fig. 1(c), considering the consistent mass distribution along the link. In this section, a type of modeling shown in Fig. 1(c) is described.

1. Formulation using Bernoulli-Euler beam elements The order of the displacement function used for the Bernoulli-Euler beam element is higher than that of the linear Timoshenko beam element, and thus, it can express deformation more accurately with fewer elements. In the model, the link mass is distributed consistently, in the same manner as the displacement function, and does not require an expression for the center of gravity. Note that, since the deformation of the element is defined using a higher-order function, it requires only one-element subdivision per member for infinitesimal deformation cases.

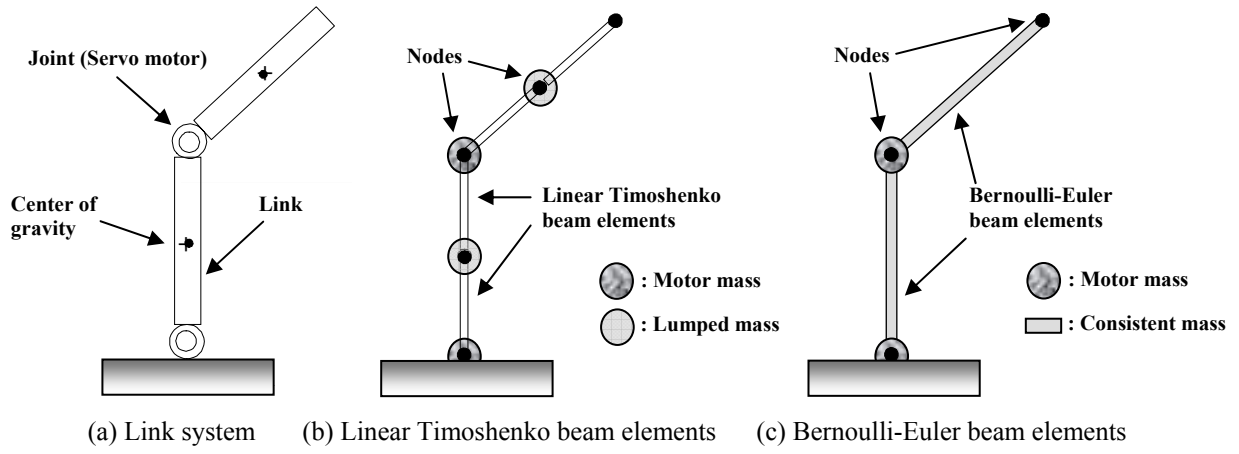


Fig. 1 Modeling of link systems using finite elements

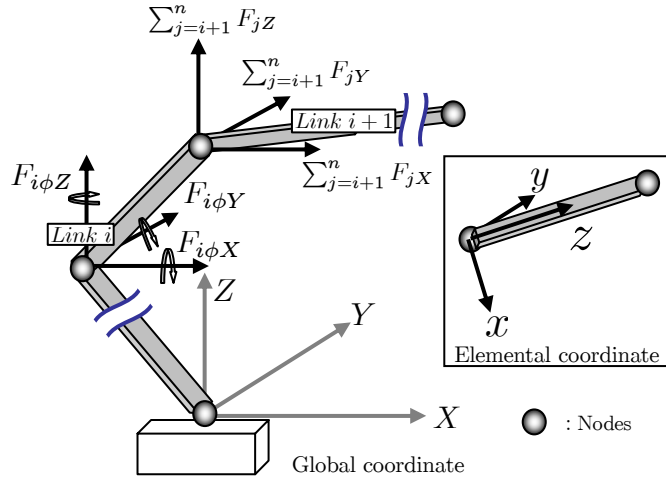


Fig. 2 Nodal forces acting in a link system with consistent mass distribution

Figure 2 shows the nodal forces (based on global coordinates) acting on the i th link in a three-dimensional open-loop n -link system with a consistent mass distribution. The joint torque τ_{ix} required around the x -elemental axis on the i th link is determined by adding the $i+1$ th joint torque $\tau_{(i+1)x}$ to the sum of the moments of inertia acting on this link, and is expressed by the nodal forces F_{iy} and $F_{i\phi x}$ based on elemental (or link) coordinates as

$$\tau_{ix} = l_i \left(\sum_{j=i+1}^n F_j \right)_y + F_{i\phi x} + \tau_{(i+1)x}. \quad (1)$$

By considering the other components around the y - and z -axes and arranging them into global coordinates (X, Y, Z) in matrix form, the joint torque vector is expressed as

$$\{\tau^n\} = [L^n][T^n]\{P^n\}, \quad (2)$$

where $\{P^n\}$ is a $6n \times 1$ vector related to nodal force, defined as

$$\{P^n\} = \begin{Bmatrix} P_1 \\ P_2 \\ \cdot \\ \cdot \\ P_n \end{Bmatrix}, \quad \text{where } \{P_i\} = \begin{Bmatrix} \sum_{j=i+1}^n F_{jX} \\ \sum_{j=i+1}^n F_{jY} \\ \sum_{j=i+1}^n F_{jZ} \\ F_{i\phi X} \\ F_{i\phi Y} \\ F_{i\phi Z} \end{Bmatrix}, \quad (i = 1, \dots, n) \quad (3)$$

2. Calculation of kinematics for flexible models To calculate the inverse dynamics for flexible models, information on target trajectories that compensate for the inertial forces acting at the links and the stiffnesses of the links is required. Therefore, a solution scheme of kinematics is developed on the basis of the FEM. Moreover, it is combined with the parallel solution scheme to handle analyzed models comprehensively in a single calculation process.

When inertia caused by the overall system motion is taken into account, the equation of motion at time $t+\Delta t$ is derived from the principle of virtual work as follows:

$$[M]\{\ddot{u}_m\}_{t+\Delta t}+[M]\{\ddot{u}_d\}_{t+\Delta t}+[C]\{\dot{u}_d\}_{t+\Delta t}+[K]\{\Delta u_d\} = \{F\}_{t+\Delta t}-\{R\}_t, \quad (10)$$

where $[M]$ is the total mass matrix, $[C]$ is the total damping matrix, $[K]$ is the total stiffness matrix, $\{F\}$ is the external force vector, and $\{R\}$ is the internal force vector. The vectors $\{\ddot{u}_m\}$ and $\{\ddot{u}_d\}$ denote the acceleration vectors for the overall system motion components and material deformation components, respectively, $\{\dot{u}_d\}$ denotes the velocity vector for material deformation components, and $\{\Delta u_d\}$ is the incremental material deformation vector at time $t+\Delta t$. By applying Newmark's β method (integration parameter: $\delta=1/2$) as a time integration scheme, the acceleration and velocity vectors are calculated as

$$\{\ddot{u}_m\}_{t+\Delta t} = \frac{1}{\beta\Delta t^2}\{\Delta u_m\} - \frac{1}{\beta\Delta t}\{\dot{u}_m\}_t - \left(\frac{1}{2\beta}-1\right)\{\ddot{u}_m\}_t, \quad (11a)$$

$$\{\ddot{u}_d\}_{t+\Delta t} = \frac{1}{\beta\Delta t^2}\{\Delta u_d\} - \frac{1}{\beta\Delta t}\{\dot{u}_d\}_t - \left(\frac{1}{2\beta}-1\right)\{\ddot{u}_d\}_t, \quad (11b)$$

$$\{\dot{u}_m\}_{t+\Delta t} = \frac{1}{2\beta\Delta t}\{\Delta u_m\} - \left(\frac{1}{2\beta}-1\right)\{\dot{u}_m\}_t - \left(\frac{1-4\beta}{4\beta}\right)\{\ddot{u}_m\}_t\Delta t, \quad (11c)$$

$$\{\dot{u}_d\}_{t+\Delta t} = \frac{1}{2\beta\Delta t}\{\Delta u_d\} - \left(\frac{1}{2\beta}-1\right)\{\dot{u}_d\}_t - \left(\frac{1-4\beta}{4\beta}\right)\{\ddot{u}_d\}_t\Delta t, \quad (11d)$$

where $\{\dot{u}_m\}$ is the velocity vector for the overall system motion components and $\{\Delta u_m\}$ is the incremental motion vector at time $t+\Delta t$. β is another integration parameter and a value of $1/4$ is used in the examples. Substituting Eq. (11) into Eq. (10) yields

$$\begin{aligned} & \left([K] + \frac{1}{\beta\Delta t^2}[M] + \frac{1}{2\beta\Delta t}[C]\right)\{\Delta u_d\} = \{F\}_{t+\Delta t} - \{R\}_t + [M]\left(\frac{1}{\beta\Delta t}\{\dot{u}_d\}_t + \left(\frac{1}{2\beta}-1\right)\{\ddot{u}_d\}_t\right) \\ & - [M]\left(\frac{1}{\beta\Delta t^2}\{\Delta u_m\} - \frac{1}{\beta\Delta t}\{\dot{u}_m\}_t - \left(\frac{1}{2\beta}-1\right)\{\ddot{u}_m\}_t\right) + [C]\left(\left(\frac{1}{2\beta}-1\right)\{\dot{u}_d\}_t + \left(\frac{1-4\beta}{4\beta}\right)\{\ddot{u}_d\}_t\Delta t\right). \end{aligned} \quad (12)$$

By applying $\{\Delta u_m\}$ as the input in a time integration loop of Eq. (12) and using the vectors of Eq. (11) at time t , $\{\Delta u_d\}$ at each time step can be successively obtained. The displacement vector $\{u_m\}$ for the overall system motion components, and the displacement vector $\{u_d\}$ for the material deformation components are calculated incrementally as

$$\{u_m\}_{t+\Delta t} = \{u_m\}_t + \{\Delta u_m\}, \quad (13a)$$

$$\{u_d\}_{t+\Delta t} = \{u_d\}_t + \{\Delta u_d\}. \quad (13b)$$

The total displacement $\{u\}$ is obtained by summing both the overall system motion and material deformation components as

$$\{u\}_{t+\Delta t} = \{u_m\}_{t+\Delta t} + \{u_d\}_{t+\Delta t}. \quad (14)$$

Final target trajectories considering the effects of stiffness and damping are obtained using Eq. (14). The resultant forces acting on the elements can also be calculated using the obtained displacements.

NUMERICAL EXAMPLES OF INVERSE DYNAMICS CALCULATIONS

In this section, some numerical examples are shown on various types of link system to confirm the applicability and expansibility of the parallel solution scheme.

1. Closed-loop, structure-varying, and multibranch link systems Although special attention must be paid to the number of incremental steps, one can obtain torque curves for a closed-loop link system (see Fig. 3(a)), a structure-varying type (see Fig. 3(b)), or even for a multibranch link system (see Fig. 3(c)) without revising any part of the numerical algorithm in the parallel solution scheme [6]. This is one of the most significant advantages of using the scheme.

2. Flexible link systems A numerical test is carried out on a 5-joint link system that consists of five different stiffness links, as shown in Table 1. Damping is considered in the calculations. In Table 1, α and β are Rayleigh's damping coefficients. An initial trajectory for a rigid-body model is given in Fig. 4(a).

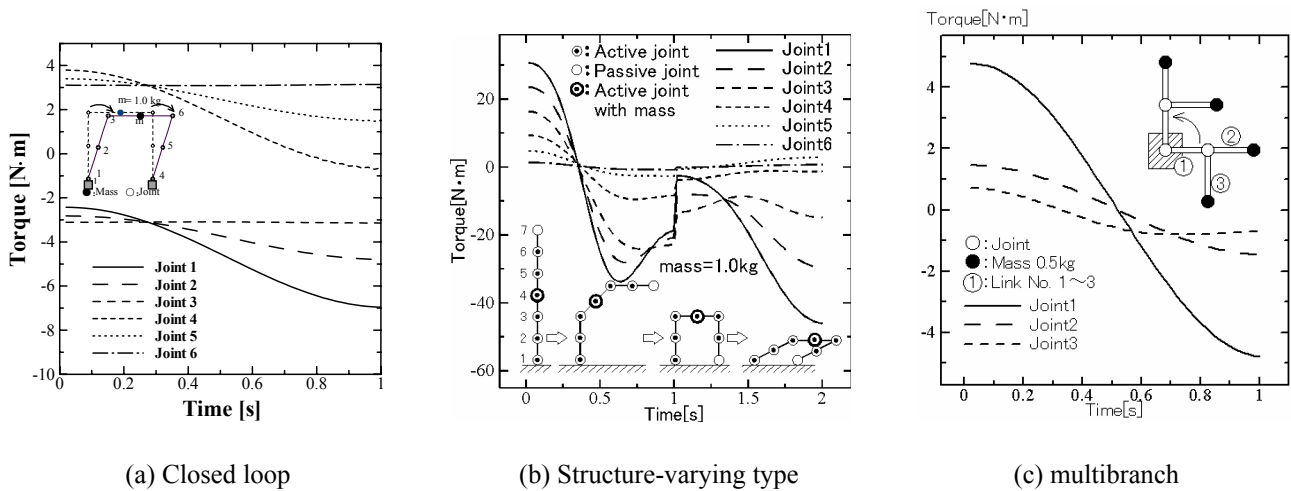


Fig. 3 Torque curves for various types of link system

Table 1. Link parameters of a five-joint flexible link system

	Link length [m]	Flexural stiffness [Nm ²]	Link mass [kg]	Extra mass [kg]	Damping coefficients	
					α	β
Link 1	0.200	0.5384	0.021	0.500	0.100	2.0×10^{-4}
Link 2	0.200	0.4376	0.021	0.200	0.100	2.0×10^{-4}
Link 3	0.200	0.2917	0.021	0.100	0.100	2.0×10^{-4}
Link 4	0.200	0.1459	0.021	0.050	0.100	2.0×10^{-4}
Link 5	0.200	0.02917	0.021	0.010	0.100	2.0×10^{-4}

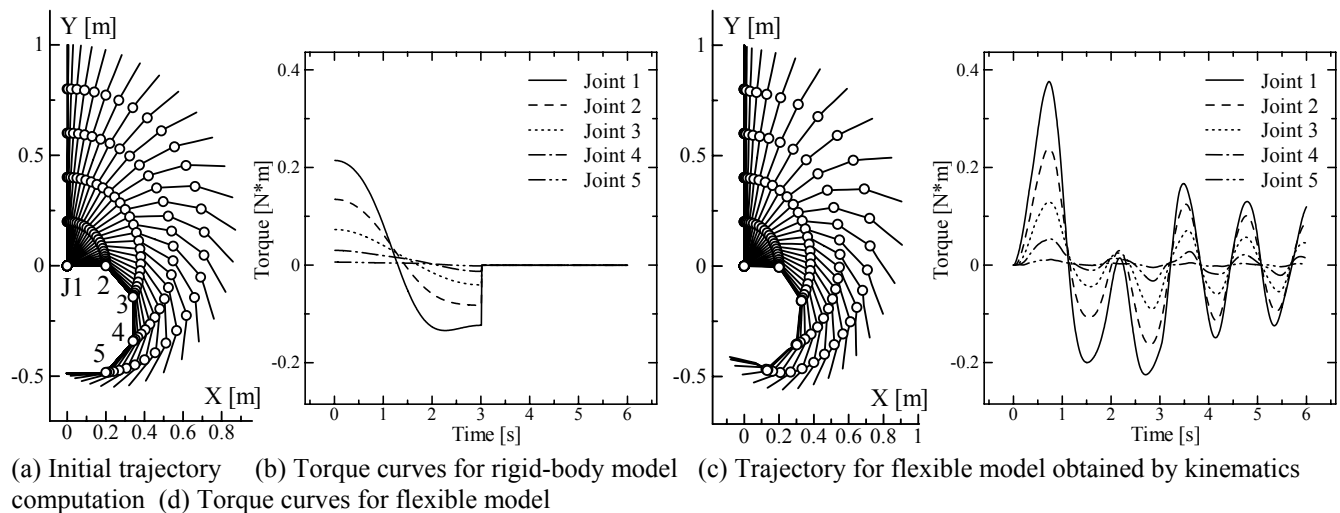


Fig. 4 Inverse dynamics calculation of a five-joint flexible link system with different stiffness values

Table 2. Link parameters of a two-joint flexible link system

Parameter	Link 1	Link 2
Link length [m]	0.25	0.25
Young's modulus [GPa]	200	4.38
Moment of inertia [m ⁴]	2.92×10^{-12}	7.72×10^{-12}
Link mass [kg]	6.83×10^{-2}	6.20×10^{-3}
Extra mass [kg]	5.81×10^{-1}	4.20×10^{-2}

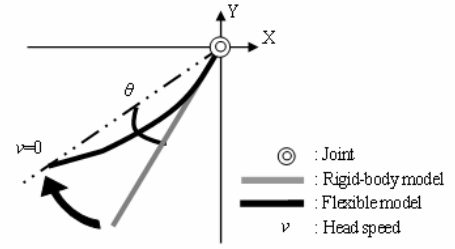


Fig. 7 Control angle for vibration control

where q and q_d are the actual angle acquired from the attached encoders and the target angle, respectively. K_P and K_I are the feedback gain for the angle and the integrated value, respectively. Values of 3.5 and 0.017 are used in the feedforward and feedback control, respectively.

Sensorless, model-based vibration control is adopted to reduce the vibration of the link head and to verify the accuracy of the calculated trajectories and torque values. The general concept of the vibration control is to rotate the base joint by a control angle θ , as shown in Fig. 7, at the instant when the link is maximally deformed after stopping. The timing of the rotation is determined by predicting the time when the speed of the link head becomes zero from the calculated trajectory. The base joint is rotated until the amplitude is sufficiently reduced. In this case, the vibration control is adopted only for Joint 2 for simplicity. Joint 1 is controlled by the trajectory without considering any oscillating motion.

The given task is a simple rotational motion, as shown in Fig. 8(a), which stops after 2 s. A trajectory for the flexible model with vibration control is obtained as shown in Fig. 8(b), from the kinematics computation. The vibration that occurs after the stop is markedly reduced. Figures 9(a) and 9(b) show a comparison of the computed and actual torques. The computed torques ($\tau_{I.D.}$) are in good agreement with the actual control torques using feedforward and feedback torques (τ_{FF+FB}) compared with the control

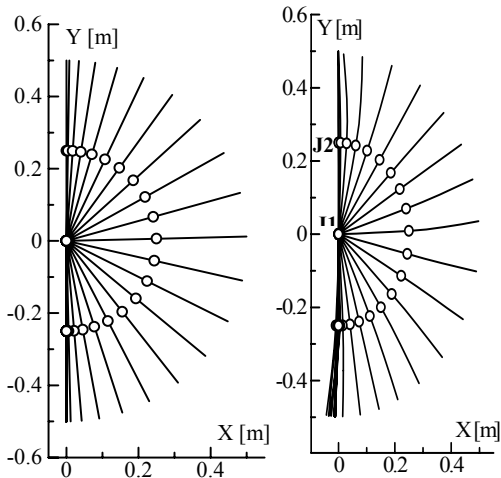
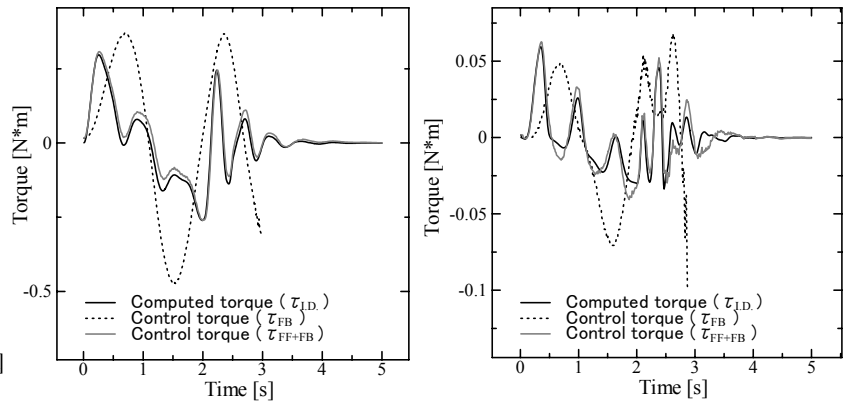


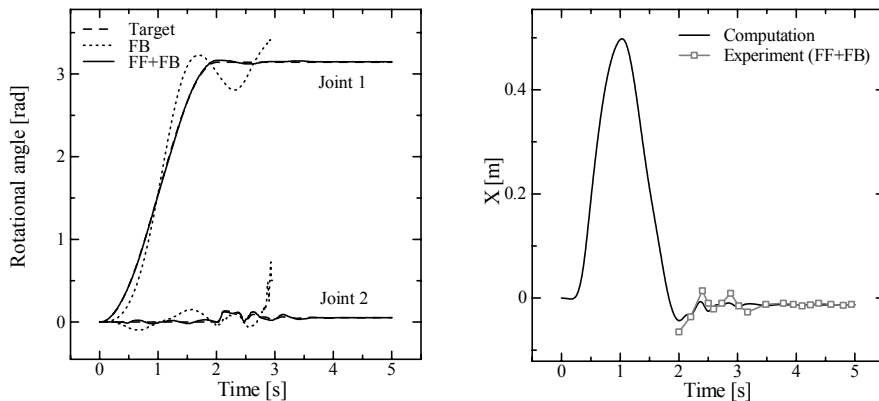
Fig. 8 Initial and obtained trajectories



(a) Joint 1

(b) Joint 2

Fig. 9 Torque curves



(a) Rotational angle

(b) X-coordinate of link head

Fig. 10 Control results

torques using only feedback torques (τ_{FB}). The complicated motion required to restrain vibration is realized in the rotational angle (Fig. 10(a)), and the computed location of the link head also agrees well with the experimental result (Fig. 10(b)). These results indicate the high accuracy of the trajectories and torque values obtained using the parallel solution scheme.

2. Seven-DOF robotic arm system Finally, some feedforward control experiments using the parallel solution scheme are carried out on a robotic arm, as shown in Fig. 11, to verify the scheme's practicability for actual robotic systems. The robotic arm [13] consists of 7-DOF joints actuated using an air cylinder, and is very light compared with an arm using 7 DC motors but has sufficient stiffness to act as an endoskeleton. The linear motion of the air cylinder is transformed to rotational motion using a screw mechanism attached to the inside of the upper arm and forearm. Input torque values are converted to air pressure values by a linear relationship. The assumed mass distribution of the mechanism is shown in Fig. 12, and it is modeled and computed explicitly using the parallel solution scheme considering the center of gravity [6]. PID feedback control is adopted, and each feedback gain is fixed to specific values throughout the experiments. One of the advantages of adopting the feedforward control is that one can restrain the feedback gains to small values. A simple 2-DOF motion is given to Joints 2 and 3, and the control results obtained are shown in Fig. 13. The computed torque curves are shown in Fig. 14. Slight delays compared with the target motion can be observed in the results, which originate from the mechanical delay caused by compressing the air cylinder. However, the positive effects of the feedforward control are apparent, particularly at the initial stage and in the overall stability. Note that although the motions are very simple, the dynamics of the system is regarded as that of a 7-DOF system, which may be very complicated to handle using conventional dynamic equations.

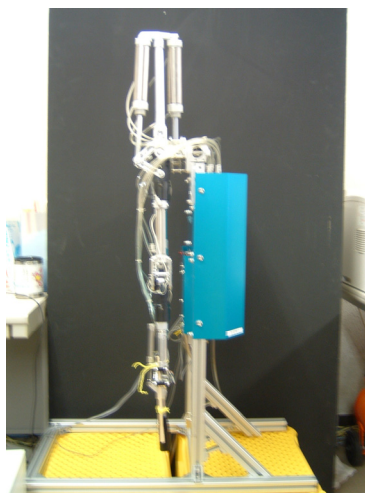


Fig. 11 Robotic arm with air cylinder used as endoskeleton [13]

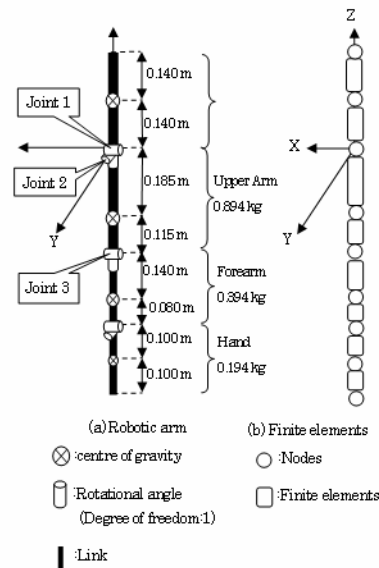
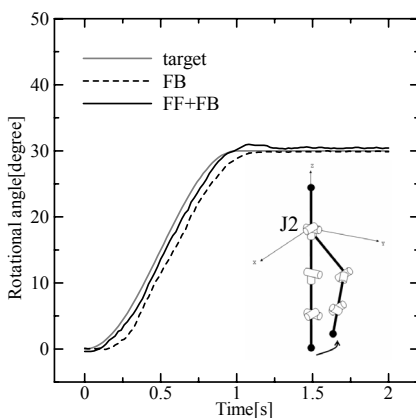
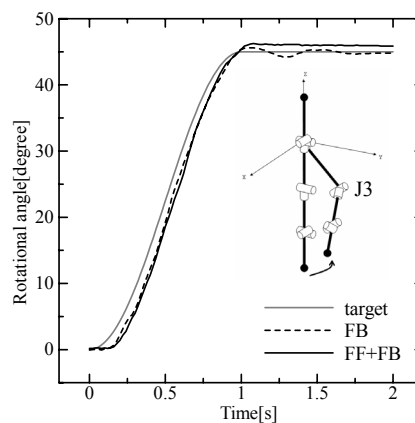


Fig. 12 Modeling of the robotic arm



(a) Joint 2



(b) Joint 3

Fig. 13 Control results for 2-DOF motion

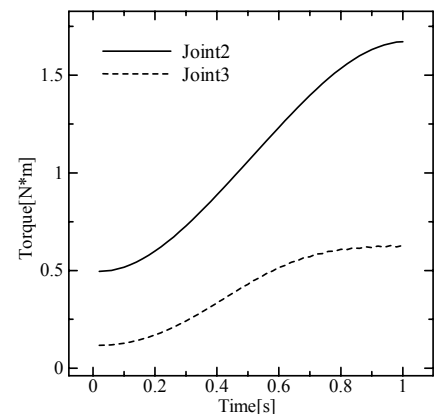


Fig. 14 Torque curves

CONCLUSION

A completely new solution scheme for calculating the inverse dynamics of robotic systems is described in this paper with various numerical examples and experimental results. The scheme derives nodal forces in parallel and converts them to a joint torque, and can easily be applied to many types of link system under various boundary conditions or with various stiffness values. The basic numerical algorithm of the scheme requires no revision for different cases. The simple algorithm enables the scheme to be more easily implemented in a program or for its functionality to be enhanced, even for nonexpert users. These advantages cannot be realized by conventional schemes based upon generally used dynamic equations. The parallel solution scheme may also be used to achieve stability and smoothness in robotic motion control. The numerical examples and control results reveal the possibility of using the scheme as a unified scheme, independent of the system configuration and physical parameters of link systems.

Acknowledgements This work was supported by Grant-in-Aid for Scientific Research (C) MEXT and the Electro-Mechanic Technology Advancing Foundation.

REFERENCES

- [1] Y. Nakamura, M. Ghodoussi, *Dynamics Computation of Closed-Link Robot Mechanisms with Nonredundant and Redundant Actuators*, IEEE Trans. Robotics and Automation, 5(3), (1989), 294-302.
- [2] K. Sugimoto, *Dynamic Analysis of Closed Loop Mechanisms on the Basis Vectors of Passive Joint Axes*, J. Robotic Systems, 20(8), (2003), 501-508.
- [3] Y. Nakamura, K. Yamane, *Dynamics Computation of Structure-Varying Kinematic Chains and Its Application to Human Figures*, IEEE Trans. Robotics and Automation, 16(2), (2000), 124-134.
- [4] D. Isobe, H. Nakagawa, *A Parallel Control System for Continuous Architecture Using Finite Element Method*, J. Intel. Mat. Syst. Structures, 9(12), (1998), 1038-1045.
- [5] D. Isobe, D. Imaizumi, Y. Chikugo, S. Sato, *A Parallel Solution Scheme for Inverse Dynamics and Its Application in Feed-forward Control of Link Mechanisms*, J. Robotics and Mechatronics, 15(1), (2003), 1-7.
- [6] D. Isobe, *A Unified Solution Scheme for Inverse Dynamics*, Advanced Robotics, 18(9), (2004), 859-880.
- [7] D. Isobe, A. Yagi, S. Sato, *General-Purpose Expression of Structural Connectivity in the Parallel Solution Scheme and Its Application*, JSME Int. J. Series C, 49(3), (2006), 789-798.
- [8] W. H. Sunada, S. Dubowsky, *On the Dynamic Analysis and Behavior of Industrial Robotic Manipulators with Elastic Members*, ASME J. Mechanisms, Transmissions, and Automation in Design, 105, (1983), 42-51.
- [9] E. Bayo, *A Finite-Element Approach to Control the End-Point Motion of a Single-Link Flexible Robot*, J. Robotic Systems, 4(1), (1987), 63-75.
- [10] A. A. Shabana, *Dynamics of Flexible Bodies Using Generalized Newton-Euler Equations*, ASME J. Dyn. Sys. Measurement Control, 112, (1990), 496-503.
- [11] R. J. Theodore, A. Ghosal, *Comparison of the Assumed Modes and Finite Element Models for Flexible Multilink Manipulators*, Int. J. Robotics Research, 14(2), (1995), 91-111.
- [12] H. Asada, Z. D. Ma, H. Tokumaru, *Inverse Dynamics of Flexible Robot Arms: Modeling and Computation for Trajectory Control*, ASME J. Dyn. Sys. Measurement Control, 112, (1990), 177-185.
- [13] Y. Koyabu, I. Kawabuchi, K. Hoshino, *Control of Humanoid Robot Arm with Air Cylinders as Endoskeletons*, Trans. Inst. Electronics, Information and Communication Engineers A, J88-A(11), (2005), 1318-1325, in Japanese.